

https://doi.org/10.3799/dqkx.2018.724



黔南基性岩墙岩石地球化学、SHRIMP 锆石 U-Pb 年代学及地质意义

祝明金¹, 田亚洲^{1*}, 聂爱国², 张恒³, 杨华燊¹

1. 贵州大学资源与环境工程学院, 贵州贵阳 550025

2. 贵州理工学院资源与环境工程学院, 贵州贵阳 550003

3. 中国地质科学院地质研究所, 北京 100037

摘要: 基性岩墙, 与层状、环状基性杂岩体和高 Ti、低 Ti 玄武岩共同组成了峨眉山大火成岩省岩石组合。为进一步确定大火成岩省及相关生物灭绝事件的时间联系, 及更深入研究大火成岩省的成因, 对分布于贵州省南部的基性岩墙进行了主、微量元素、Sr-Nd 同位素测定和锆石 SHRIMP U-Pb 年代学研究。黔南基性岩墙 $\Sigma\text{REE}=135.66\times 10^{-6}\sim 280.59\times 10^{-6}$, LREE/HREE 为 6.42~7.54, $(\text{La}/\text{Yb})_{\text{N}}$ 为 7.94~9.85, 轻重稀土分异明显, δEu 为 1.0~1.3, 具有 Ba、Sr、K 等 LILE 富集, Nb、Ta、Zr、Hf 等 HFSE 亏损特征, 显示与峨眉山高钛玄武岩相似的地球化学特征。Th/Ta(1.80~1.94)、Nb/U(30.8~39.88)、Th/La(0.08~0.10)、Nb/Th(7.89~8.40) 比值与原始地幔相似, 较低的初始 ($^{87}\text{Sr}/^{86}\text{Sr}$)_i 比值(0.705 278~0.706 052)、 $\epsilon_{\text{Nd}}(t)$ (-0.5~+1.6)、以及 Th/Ta 比值(<2.13) 显示岩浆无明显的地壳混染, 岩浆可能形成于受地幔柱作用的富集石榴石地幔源区 10%~12% 的部分熔融。SHRIMP 锆石 $^{206}\text{Pb}/^{238}\text{U}$ 加权平均年龄为 261.2 ± 2.6 Ma, 反映峨眉山大火成岩的喷发时间可能集中在 260 Ma 左右, 并可能与瓜德鲁普末期的生物灭绝有关。

关键词: 基性岩墙; 岩石学; 地球化学; SHRIMP 锆石 U-Pb 年龄; 峨眉山大火成岩省; 黔南。

中图分类号: P581

文章编号: 1000-2383(2018)04-1333-17

收稿日期: 2017-12-20

Petrogeochemistry, Zircon SHRIMP U-Pb Geochronology of Mafic Dykes in South Guizhou and Their Geological Implications

Zhu Mingjin¹, Tian Yazhou^{1*}, Nie Aiguo², Zhang Heng³, Yang Huashen¹

1. College of Resources and Environmental Engineering, Guizhou University, Guiyang 550025, China

2. College of Resources and Environmental Engineering, Guizhou Institute of Technology, Guiyang 550003, China

3. Institute of Geology, Chinese Academy of Geological Sciences, Beijing 100037, China

Abstract: The rocks of Emeishan large igneous province (ELIP) are mainly composed of mafic dykes, layered and ring mafic complex, high Ti and low Ti basalts. The major elements, trace elements, Sr-Nd isotopes and zircon SHRIMP U-Pb ages of mafic dykes from South Guizhou Province were studied in order to further determine the temporal link between ELIP and related mass extinction events and research the genesis of ELIP in this paper. Results show $\Sigma\text{REE}=135.66\times 10^{-6}\sim 280.59\times 10^{-6}$, LREE/HREE=6.42~7.54, $(\text{La}/\text{Yb})_{\text{N}}=7.94\sim 9.85$, relatively enriched LREE to HREE, $\delta\text{Eu}=1.0\sim 1.3$, enriched LILE, such as Ba, K, Sr, depleted HFSE, such as Nb, Ta, Zr, Hf, displaying similar geochemical characteristics of Emeishan high Ti basalts. The similar ratios of Th/Ta(1.80~1.94), Nb/U(30.8~39.88), Th/La(0.08~0.10), Nb/Th(7.89~8.40) to

基金项目: 贵州大学人才引进项目(No.702400163301); 贵州理工学院高层次人才科研启动经费项目(No.XJGC20140702); 国家自然科学基金(Nos.41703036, 41262005)。

作者简介: 祝明金(1986-), 男, 博士研究生, 矿物学、岩石学、矿床学专业。ORCID: 0000-0002-7824-1176. E-mail: zhumingjin@outlook.com

* **通讯作者:** 田亚洲, ORCID: 0000-0002-9246-515X. E-mail: tianyazhou87@163.com

引用格式: 祝明金, 田亚洲, 聂爱国, 等, 2018. 黔南基性岩墙岩石地球化学、SHRIMP 锆石 U-Pb 年代学及地质意义. 地球科学, 43(4): 1333-1349.

primitive mantle, low ($^{87}\text{Sr}/^{86}\text{Sr}$)_i (0.705 278–0.706 052), $\epsilon_{\text{Nd}}(t)$ (–0.5~+1.6) and Th/Ta (<2.13) imply no obvious crustal contamination, and the mafic rocks may have been caused by 10%–12% partial melting of the garnet peridotite in their source region that interacted with the upwelling Emeishan plume at the periphery of the plume. The 261.2 ± 2.6 Ma age of zircon SHRIMP U-Pb may imply that the ELIP formed by a mantle plume at ~260 Ma and was one of the likely causes of the end-Guadalupian mass extinction.

Key words: mafic dyke; petrology; geochemistry; zircon SHRIMP U-Pb age; Emeishan large igneous province; South Guizhou.

0 引言

峨眉山大火成岩省因其典型的地幔柱成因标志、含有世界级的 V-Ti-Fe 矿床以及与生物灭绝的时间耦合等,吸引了一大批学者对其形成时代、规模(分布面积和体积)、形成机制和过程、生物灭绝机制等方面进行研究。尽管前人在矿床学、岩石学、地球化学及生物地质学方面做了大量研究,但对于大火成岩省的喷发时限一直都存在争议。早期对峨眉山大火成岩省年龄的测试方法主要为 Ar-Ar 同位素测年(Lo *et al.*, 2002; Boven *et al.*, 2002; Fan *et al.*, 2004),年龄小于 256 Ma,认为峨眉山大火成岩省形成于二叠纪末。但这些数据随后遭到 Ali *et al.* (2004, 2005)和 He *et al.* (2007)的质疑,认为这可能受到后期构造热事件的扰动。自 Zhou *et al.* (2002)对新街岩体辉长岩进行锆石 SHRIMP U-Pb 定年以来,对与玄武岩同期的侵入岩体或脉体的高精度锆石 U-Pb 定年(SHRIMP 或 TIMS)多集中在 260 Ma,而一些小于 260 Ma 的岩浆事件被认为与地幔柱传导加热所导致的地壳滞后的熔融有关(Zhong *et al.*, 2007; Xu *et al.*, 2008)。二叠纪共有两次生物灭绝,一次为中二叠纪晚期至晚二叠纪早期,即瓜德鲁普末期的生物灭绝(Jin *et al.*, 1994),另一次为二叠纪—三叠纪边界的生物灭绝事件(PTB)(Erwin, 1994)。测年对象多为与峨眉山玄武岩同源的基性—超基性侵入岩,代表峨眉山大火成岩省的形成年龄在 260 Ma 左右,与瓜德鲁普末期的生物灭绝时间耦合,说明两者可能有成因联系。但 Re-Os 同位素体系、锆石 LA-ICP-MS U-Pb 定年所得的年龄普遍较小,部分学者认为这些年龄可能代表了峨眉山大火成岩省主要与二叠纪—三叠纪生物灭绝有关(王登红等, 2007; 朱江等, 2011)。年龄上的分歧使得峨眉山大火成岩省与二叠纪生物灭绝的时间关系变得模糊。因此,确定大火成岩省末期的精确时间变得尤为重要,是区分峨眉山大火成岩省与二叠纪哪一次生物灭绝有关的关键证据。

峨眉山大火成岩省的岩石组合主要包括基性岩墙、层状、环状基性杂岩体和高 Ti、低 Ti 玄武岩。放射性岩墙群作为鉴别古老地幔柱的标志之一(Campbell, 2007; Li *et al.*, 2015),常分布于大火成岩省的外围区域,在峨眉山大火成岩省中也广有分布。李宏博等(2010)以及 Li *et al.* (2015)在峨眉山大火成岩省中识别出 6 条辐射角近 200°的基性岩墙群。贵州西部分布有 5 条,分别为毕节岩墙群、威宁岩墙、白沙岩墙、盘县岩墙和罗甸岩墙。以往的研究多集中在攀西地区,但针对基性岩墙群的研究却不多。李宏博(2012)以及 Li *et al.* (2015)测得云南富民辉绿岩的锆石 LA-ICP-MS 年龄为 257.6 ± 2 Ma,同位素特征指示与高钛玄武岩成因相似,四川冕宁基性岩墙的年龄为 256.7 ± 4.3 Ma,认为代表大火成岩省大规模活动过程的末期。贵州基性岩墙的研究程度较低,曾广乾等(2014)对普安辉绿岩进行了主量、微量和锆石 LA-ICP-MS U-Pb 定年分析,认为普安辉绿岩高钛,具 OIB 特征,与峨眉山玄武岩同源,且年龄为 263 ± 10 Ma,代表了地幔柱的启动时间。韩伟等(2009)通过分析贵州罗甸基性岩的主微量元素和锆石 LA-ICP-MS U-Pb 定年,认为基性岩墙具有与峨眉山玄武岩相似的地球化学性质,其年龄 255 Ma 代表了玄武岩的主喷发期。锆石 LA-ICP-MS U-Pb 定年由于分析过程中受人为干扰的可能性较大,分析误差范围较大,可达 10 Ma(Shellnutt *et al.*, 2012)。因此,更加精确的同位素年代学测试方法可获得更加真实的年龄数据。

黔南基性岩墙位于峨眉山大火成岩省的东缘地带,缺乏高精度锆石 U-Pb 年代学数据,制约了对峨眉山大火成岩省喷发时限和对大火成岩省与生物灭绝的时间联系的认知。同时,对这些基性岩墙进行详细的主、微量元素、稀土元素和同位素地球化学研究,有助于了解峨眉山大火成岩省东部边缘地区的岩浆源区性质以及地幔柱活动过程,有利于更深化研究大火成岩省的成因。本文基于对黔南基性岩墙详细的岩石地球化学分析以及 SHRIMP 锆石 U-Pb 精

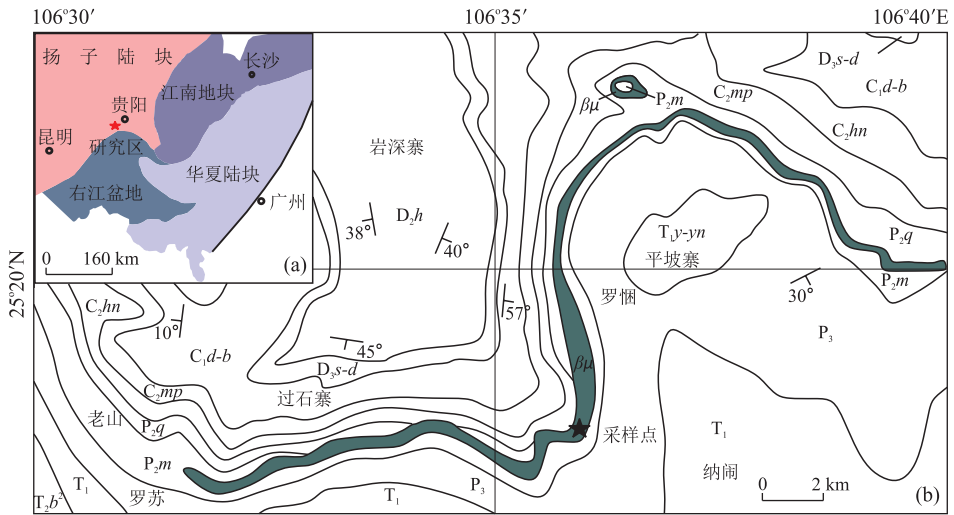


图 1 黔南基性岩墙地质图

Fig.1 Geological background of the mafic dyke, South Guizhou

a. 研究区大地构造位置图, 据程裕淇(1994); b. 黔南基性岩墙地质略图, 据 1:20 万罗甸幅(贵州省地质局 108 队, 1965; 1:20 万罗甸幅)、乐业幅地质图(广西壮族自治区地质局, 1972; 1:20 万乐业幅地质图)修改。T₂b². 中三叠统边阳组中段; T₁. 下三叠统; P₂m. 中二叠统茅口组; P₂q. 中二叠统栖霞组; C₂mp. 上石炭统马平组; C₂hn. 上石炭统黄龙组; C₁d-b. 下石炭统大塘组—摆佐组; D₃s-d. 上泥盆统响水洞组—一代化组; D₂h. 中泥盆统火烘组; βμ. 基性岩墙

确定年, 探讨基性岩墙成因、形成时代以及峨眉山大火成岩省的喷发时限。

1 地质背景

1.1 区域地质

研究区位于扬子陆块西南缘与右江盆地的交汇部位(图 1a), 早泥盆世晚期至二叠纪, 桑郎—罗甸断裂带作为右江陆缘裂谷系北缘的一条同生伸展型断槽, 控制了槽盆相沉积及其两侧台地相沉积的岩相分界, 为基性岩群的侵位活动提供了良好的构造就位空间, 形成了切割深度已达上地幔顶部的岩石圈型深断裂带(王尚彦等, 2005)。同时, 岩墙位于峨眉山大火成岩省分布的外带。属李宏博等(2010)所划分的与大火成岩省有关的基性岩墙群的 III 号岩墙群(图 2), 峨眉山大火成岩省位于扬子地台西缘, 主要由大量溢流玄武岩和同时期的基性—超基性侵入岩以及长英质岩体组成, 还含有少量苦橄岩、粗面岩、粗安岩、熔结凝灰岩, 被认为与地幔柱活动有关(Chung and Jahn, 1995; Xu *et al.*, 2001, 2004; He *et al.*, 2003; Zhang, 2006a, 2006b; Zhang *et al.*, 2008)。溢流玄武岩覆盖面积约 $2.5 \times 10^5 \text{ km}^2$, 厚度从西部 5 000 多米到东部贵州境内的几百米, 平均厚度约 700 m, 体积约 $0.3 \times 10^6 \text{ km}^3$ (Xu *et al.*, 2001)。火成岩省呈菱形分布, 龙门山逆冲断裂和哀

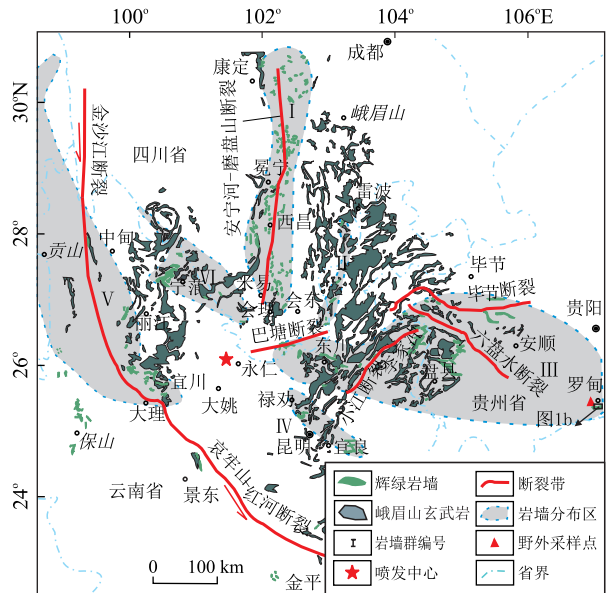


图 2 ELIP 基性岩墙群分布及采样位置

Fig.2 Distribution of ELIP mafic dyke swarms and sample location

据李宏博等(2010)

牢山—红河走滑断裂分别为峨眉山大火成岩省的西北和西南边界, 后期的断裂错动使得在西藏羌塘地块和越南北部都分布有峨眉山大火成岩省的部分(Pearce and Mei, 1988; 肖龙等, 2003)(图 2)。

1.2 岩体地质

区内构造样式主要表现为北西向、北东向以及

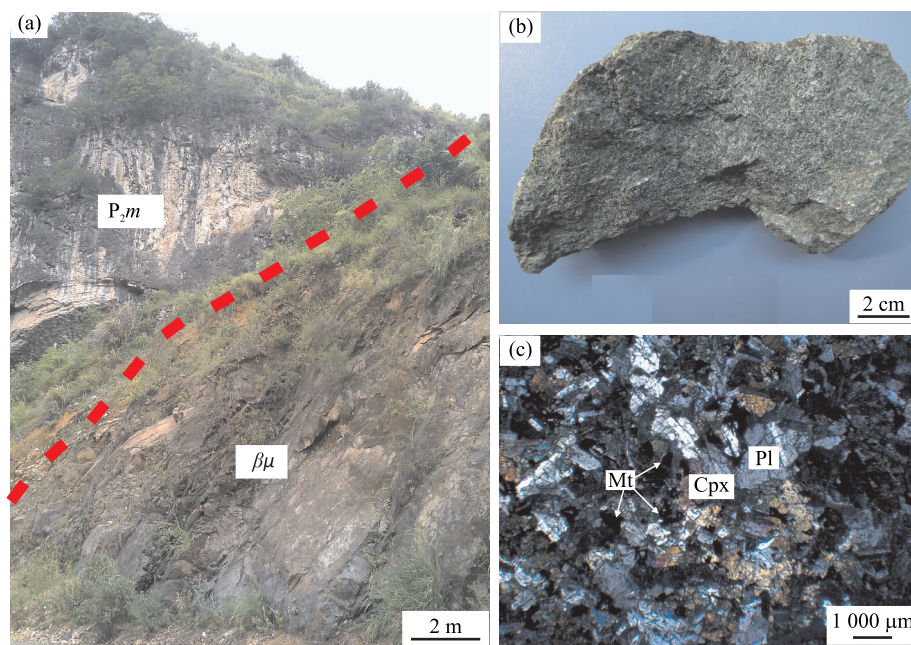


图 3 基性岩墙野外露头(a)、手标本(b)以及正交偏光镜下特征(c)

Fig.3 Photos of the outcrops (a), hand specimen (b) and microscope of the mafic dyke in cross-polarized light (c)

Pl.斜长石;Cpx.单斜辉石;Mt.磁铁矿

近东西向,其中断裂与褶皱均较发育,褶皱叠加现象明显.出露的地层主要有泥盆系、石炭系、二叠系、三叠系和第四系.区内岩浆岩类型简单,主要发育基性岩墙,分布于贵州省南部罗甸一望漠一带,NE-SW向展布,岩墙出露宽度 15~315 m,一般为 100~200 m,总体为顺层侵入于中二叠统茅口组地层中,倾向与岩层基本一致,倾角一般为 50°~60°,邻区局部可见基性岩侵入于中二叠统栖霞组和上石炭统地层中(图 1b).

本次所采样品 LK1 位于贵州省南部罗甸县罗悃镇,GPS 坐标为 N25°18'50"、E106°36'12",所采样品选取岩墙中部相对新鲜未蚀变的深灰绿色岩石,且手标本上长石结晶颗粒相对较大的岩石用于挑选锆石(图 3a,3b).对岩石薄片进行镜下鉴定,其主要组成矿物有斜长石、单斜辉石和磁铁矿,矿物较新鲜(图 3c).杂乱排列的自形和半自形的斜长石间有他形的单斜辉石和磁铁矿充填,具有典型的辉绿结构,长石和辉石均遭受一定程度的后期蚀变.斜长石多呈板状,长 500~1 000 μm 之间,含量为 60%~70%;单斜辉石多呈他形粒状,粒径在 200~1 000 μm 之间,含量为 25%~35%;磁铁矿主要呈他形不规则状分布,粒径多小于 500 μm ,含量小于 5%.黔南基性岩与灰岩接触带附近透闪石化和大理岩化强烈,为罗甸软玉矿的赋矿地层.

2 分析测试方法

2.1 主量、稀土和微量元素

样品主量、微量元素和稀土元素分析测试在广州澳实分析检测中心完成.主量元素采用 XRF 分析获得,各项元素的分析精度(RSD) SiO_2 为 0.8%, Al_2O_3 为 0.5%, Fe_2O_3 为 0.4%, MnO 为 0.7%, MgO 为 0.7%, CaO 为 0.6%, Na_2O 为 0.3%, K_2O 为 0.4%, P_2O_5 为 0.8%, TiO_2 为 0.9%.稀土和微量元素在 Finigan MAT 制造的 HR-ICP-MS(Element I)仪器上完成,采用 HF+ HNO_3 密封溶解,然后加入 Rh 内标溶液,再用 1% HNO_3 定容.实验测试过程中温度为 20 $^\circ\text{C}$,湿度为 30%,含量大于 10×10^{-6} 时相对误差小于 5%,含量小于 10×10^{-6} 时相对误差小于 10%.详细测试方法参见何红蓼等(2002).

2.2 Rb-Sr、Sm-Nd 同位素

Rb-Sr、Sm-Nd 同位素分析在中国科学技术大学放射性成因同位素地球化学实验室完成.准确地称取粉末样品 100 mg 左右放置于 15 mL 的 Teflon 闷罐中,滴入 8~10 滴纯化 HClO_4 摇匀后,加入 2~3 mL 纯化 HF,密闭加热一周左右以充分溶解样品.Rb-Sr 同位素和 REE 分离纯化在装有 5 mL AG50W-X12 交换树脂(200~400 目)的石英交换柱中完成,Sm-Nd 同位素的分离纯化在装有 1.7 mL

Teflon 粉末的石英交换柱中完成。同位素比值的测试在 MAT-262 热电离质谱计完成, Rb-Sr 同位素比值测定采用 Ta 金属带和 Ta 发射剂; Sm-Nd 同位素比值测定采用 Re 金属带。测量得到的同位素比值采用 $^{86}\text{Sr}/^{88}\text{Sr}=0.119\ 4$ 和 $^{146}\text{Nd}/^{144}\text{Nd}=0.721\ 9$ 进行质量分馏校正。标准溶液 NBS987 长期的测量结果为 $^{87}\text{Sr}/^{86}\text{Sr}=0.710\ 249\pm 0.000\ 012(2\sigma, n=38)$, 标准溶液 La Jolla 长期的测量结果为 $^{143}\text{Nd}/^{144}\text{Nd}=0.511\ 869\pm 0.000\ 006(2\sigma, n=25)$ 。同位素比值测量精度优于 0.003% 。全岩 Sr、Nd 同位素分析的全流程本底值分别是 $<200\times 10^{-12}\text{ g}$ 、 $<100\times 10^{-12}\text{ g}$ 。详细同位素分析流程参见 Chen *et al.* (2000, 2002)。

2.3 SHRIMP 锆石 U-Pb 年龄测定

前期采集 20 kg 新鲜岩石样品至河北廊坊宇恒岩矿技术服务有限公司进行锆石挑选。将锆石颗粒和锆石标样粘贴于环氧树脂靶中进行打磨抛光, 使其露出一半晶面。对锆石进行投射光、反射光以及阴极发光 (CL) 显微照相, 挑选出内部颗粒较大、清晰、无包体、无裂纹区进行测年 (宋彪等, 2002; 陈文等, 2011), 以上步骤在北京离子探针中心扫描电镜实验室完成。锆石 U-Pb 年龄测定在北京离子探针中心 SHRIMP II 仪器上完成, 详细分析流程见 Lance *et al.* (2003a, 2003b)。年龄测定仪器质量分辨率约为 5 000 (1% 峰高), 一次离子流 O_2^- 强度为 4 nA, 一次离子流束斑直径为 30 μm 左右。每个数据点测定由 5 次扫描构成, 分别采用标准锆石 TEM 和 M257 进行元素间的分馏校正和 U、Th、Pb 含量标定。其中 TEM 具有 U-Pb 谐和年龄, U、Th、Pb 含量不均一。原始数据处理和锆石 U-Pb 谐和图的绘制采用 Ludwig 编写的 Squid 和 Isoplot 程序 (Ludwig, 2001)。普通铅校正根据实测的 ^{204}Pb 进行, 普通铅的组成根据 Stacey 给出的模式计算得到 (Stacey and Kramers, 1975)。

3 数据结果

3.1 基性岩墙岩石地球化学特征

10 个样品全岩地球化学分析结果见表 1。样品主量元素分析结果在扣除烧失量之后进行归一化, 以下作图和结论均按归一化后的“干”成分进行。

3.1.1 主量元素特征 10 个样品主量元素含量去除烧失量, 归一化到 100% 后, SiO_2 含量为 45.56%~49.35%, Al_2O_3 含量为 12.36%~16.37%, 全铁 FeO^T 含量为 14.57%~16.88%,

MnO 含量为 0.17%~0.28%, MgO 含量为 4.15%~6.11%, CaO 含量为 6.93%~11.08%, Na_2O 含量为 3.88%~4.78%, K_2O 含量为 0.46%~41.37%, P_2O_5 含量为 0.56%~1.11%, TiO_2 含量为 2.91%~3.74%, 与 Xu *et al.* (2001) 定义的峨眉山高钛玄武岩 TiO_2 含量相当。样品烧失量在 1.55%~3.42% 之间, 表明岩石形成后遭受到一定的热液蚀变, 与样品薄片观察到长石和辉石的蚀变现象一致。在 TAS 岩石分类图解 (图 4a) 中, 分析数据点落入碱性系列的玄武岩和玄武粗面岩范围内, 在抗蚀变元素 $\text{Nb/Y-Zr}/\text{TiO}_2\times 0.000\ 1$ 岩石分类图解中 (图 4b), 所有数据点均落入碱性玄武岩区, 因此, 黔南基性岩墙为高 Ti 系列碱性基性岩。Harker 图解 (图 5) 显示, 样品 SiO_2 与 MgO 和 CaO 具有负相关关系, 在 SiO_2 含量大于 47% 后, 与 TiO_2 、 P_2O_5 有正相关关系, 与热液活动中不活动元素 Th、Yb 和 Zr 也具有正相关关系。 MgO 与 Ni 具有正相关性。

3.1.2 微量和稀土元素特征 基性岩墙的 $\Sigma\text{REE}=135.66\times 10^{-6}\sim 280.59\times 10^{-6}$, LREE/HREE 为 6.42~7.54, $(\text{La}/\text{Yb})_N$ 为 7.94~9.85, 轻重稀土分异明显, δEu 为 1.0~1.3。在球粒陨石 REE 配分曲线中 (图 6a), 显示 LREE 富集, 稀土配分曲线与峨眉山高钛玄武岩相似。原始地幔标准化蛛网图解中 (图 6b), 罗甸基性岩显示 Ba、Sr、K 等 LILE 富集, Nb、Ta、Zr、Hf 等 HFSE 亏损, 除 P 以外, 显示与峨眉山高钛玄武岩相似的微量元素特征。

3.1.3 Sr-Nd 同位素特征 10 个样品 Sr-Nd 同位素数据见表 2。基性岩 $(^{87}\text{Sr}/^{86}\text{Sr})_i$ 变化范围较窄, 为 0.705 278~0.706 052, $\epsilon_{\text{Nd}}(t)$ 在 -0.5~+1.6 之间, Sr-Nd 同位素均落入峨眉山玄武岩范围内 (图 7)。

3.2 锆石年代学

10 粒锆石 SHRIMP U-Pb 测试结果见表 3。表 3 年龄的误差为 1σ 绝对误差, 同位素比值的误差为 1σ 相对误差; 文中所使用 $^{206}\text{Pb}/^{238}\text{U}$ 年龄加权平均值为 95% 的置信度误差。锆石自形程度较好, 多为自形和半自形, 但粒度较小, 粒径多小于 100 μm 。阴极发光 (CL) 图像显示锆石震荡环带结构不明显, 总体较暗, 核幔结构不发育 (图 8), 与其 U、Th 含量较高有关。10 个点的年龄数据显示, 锆石的 U、Th 含量变化较大, 两者的含量变化分别介于 $497\times 10^{-6}\sim 3\ 077\times 10^{-6}$ 和 $469\times 10^{-6}\sim 3\ 283\times 10^{-6}$, Th/U 比值在 0.97~4.02 之间变化 (表 1), 均大于 0.4, 显示岩浆成因的锆石特征 (Belousova *et al.*, 2002)。10 个点年龄较为集中, 成群分布于谐和曲线上或附

表 1 黔南基性岩墙岩石主量元素(%)、微量和稀土元素(10^{-6})化学成分分析结果Table 1 Major (%) and trace and REE element (10^{-6}) abundances for the mafic dyke from South Guizhou

样号	GG14-1	GG14-2	QJ1-1	ec7	ec8	ec10	BS2	BS5	LM1	LM4
SiO ₂	47.00	46.20	45.50	45.80	47.50	48.50	46.00	45.50	44.40	46.80
TiO ₂	3.10	3.28	3.29	2.81	3.65	3.63	2.79	2.83	3.25	3.65
Al ₂ O ₃	12.90	13.05	14.10	14.15	12.45	12.55	15.70	15.60	13.95	12.05
Fe ₂ O ₃	15.60	15.50	14.92	14.08	16.36	14.33	13.98	14.72	14.76	16.46
MnO	0.23	0.21	0.22	0.19	0.27	0.19	0.16	0.18	0.20	0.27
MgO	5.52	4.32	6.02	5.24	4.05	5.64	4.48	4.70	5.80	4.90
CaO	7.51	9.22	10.00	9.20	6.76	7.35	7.61	8.22	10.80	8.24
Na ₂ O	4.25	3.98	2.63	3.57	4.08	4.70	3.72	3.68	2.93	3.07
K ₂ O	0.75	1.06	1.18	0.59	1.34	0.45	0.94	0.99	0.64	1.10
P ₂ O ₅	0.76	0.84	0.71	0.71	1.08	0.93	0.54	0.57	0.73	0.95
LOI	2.42	1.91	1.74	2.88	1.59	1.55	3.42	2.86	2.48	2.00
Total	100.04	99.57	100.31	99.22	99.13	99.82	99.34	99.85	99.94	99.49
Rb	13.40	18.00	21.40	9.70	22.70	8.30	22.90	23.90	7.30	22.50
Sr	454	916	606	602	332	437	596	663	694	708
Ba	340	440	640	270	570	360	490	490	1860	600
Th	2.50	3.20	2.80	2.70	3.90	3.40	1.80	1.90	2.60	3.50
U	0.60	0.70	0.70	0.60	0.80	0.80	0.40	0.50	0.60	0.80
Nb	21.00	25.90	22.10	21.60	31.90	27.20	15.10	15.40	21.70	29.40
Ta	1.36	1.68	1.46	1.44	2.17	1.81	0.97	0.98	1.43	1.89
Pb	2.10	7.10	2.60	1.30	3.00	2.00	2.00	1.90	1.60	4.40
Zr	106.50	129.00	150.00	98.10	130.50	146.50	77.60	83.00	125.00	152.50
Hf	3.20	3.80	3.90	2.90	3.90	4.10	2.30	2.40	3.70	4.20
Ti	18 585	19 664	19 724	16 846	21 882	21 762	16 726	16 966	19 484	21 882
Ni	39.30	25.10	81.60	35.50	7.50	20.80	59.80	66.50	83.90	6.30
V	311	367	345	310	297	343	362	404	344	335
La	30.50	35.50	27.60	30.70	49.70	37.80	22.90	23.10	29.40	43.10
Ce	69.00	80.10	62.70	68.50	110.00	88.40	51.20	52.60	67.00	97.90
Pr	8.80	10.10	8.25	8.88	14.05	11.40	6.66	6.77	8.41	12.30
Nd	37.80	42.80	33.60	36.90	58.00	47.50	27.80	28.70	35.30	51.20
Sm	8.01	8.84	7.08	7.89	11.70	10.30	6.37	6.24	7.54	10.85
Eu	3.11	3.66	3.13	2.93	4.17	3.30	2.45	2.42	3.11	3.92
Gd	7.87	8.72	6.93	7.60	11.45	9.95	6.21	6.06	7.12	10.50
Tb	1.11	1.23	0.89	1.09	1.60	1.34	0.91	0.85	0.93	1.46
Dy	6.12	7.03	5.23	6.12	8.97	7.48	4.87	4.98	5.44	8.42
Ho	1.19	1.34	1.02	1.20	1.69	1.48	0.95	0.98	1.02	1.62
Er	3.32	3.79	2.50	3.32	4.46	4.01	2.56	2.34	2.60	4.23
Tm	0.42	0.45	0.34	0.44	0.61	0.49	0.36	0.33	0.35	0.51
Yb	2.50	3.08	2.15	2.52	3.62	3.24	2.07	1.93	2.20	3.43
Lu	0.40	0.47	0.32	0.40	0.57	0.50	0.35	0.31	0.33	0.49
Y	30.50	35.10	26.70	31.10	42.90	38.70	23.90	23.50	26.60	40.20
δ Eu	1.20	1.27	1.37	1.16	1.10	1.00	1.19	1.20	1.30	1.12
Σ REE	180.15	207.11	161.74	178.49	280.59	227.19	135.66	137.61	170.75	249.93
LREE/HREE	6.86	6.93	7.35	6.87	7.51	6.97	6.42	6.74	7.54	7.15
(La/Yb) _N	8.75	8.27	9.21	8.74	9.85	8.37	7.94	8.59	9.59	9.01
Th/Ta	1.84	1.90	1.92	1.88	1.80	1.88	1.86	1.94	1.82	1.85
Nb/U	35.00	37.00	31.57	36.00	39.88	34.00	37.75	30.80	36.17	36.75
Th/La	0.08	0.09	0.10	0.09	0.08	0.09	0.08	0.08	0.09	0.08
Nb/Th	8.40	8.09	7.89	8.00	8.18	8.00	8.39	8.11	8.35	8.40
La/Nb	1.45	1.37	1.25	1.42	1.56	1.39	1.52	1.50	1.35	1.47

近, $^{206}\text{Pb}/^{238}\text{U}$ 表面年龄加权平均值为 261.9 ± 2.1 Ma ($n=10$, MSWD=1.4), 该年龄代表了基性岩中锆石的结晶年龄, 即基性岩的形成年龄。

4 讨论

4.1 基性岩墙成因

罗甸基性岩的主、微量元素和稀土元素显示与峨眉山高钛玄武岩相似的地球化学特征, 一般认为

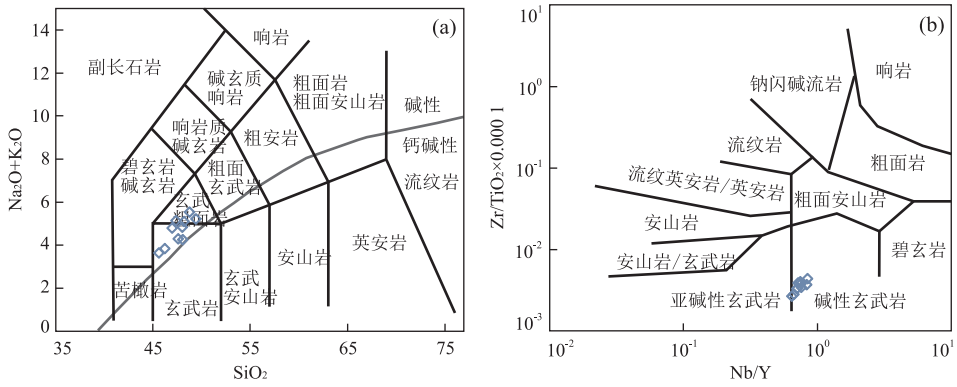


图 4 黔南基性岩墙 SiO₂-K₂O+Na₂O 图解(a)和 Nb/Y-Zr/TiO₂ × 0.000 1 图解(b)

Fig.4 SiO₂ vs. K₂O+Na₂O (a), and Nb/Y-Zr/TiO₂ × 0.000 1 (b) for the mafic dyke from South Guizhou

图 a 据 Bas *et al.*(1986); 图 b 据 Winchester and Floyd(1977)

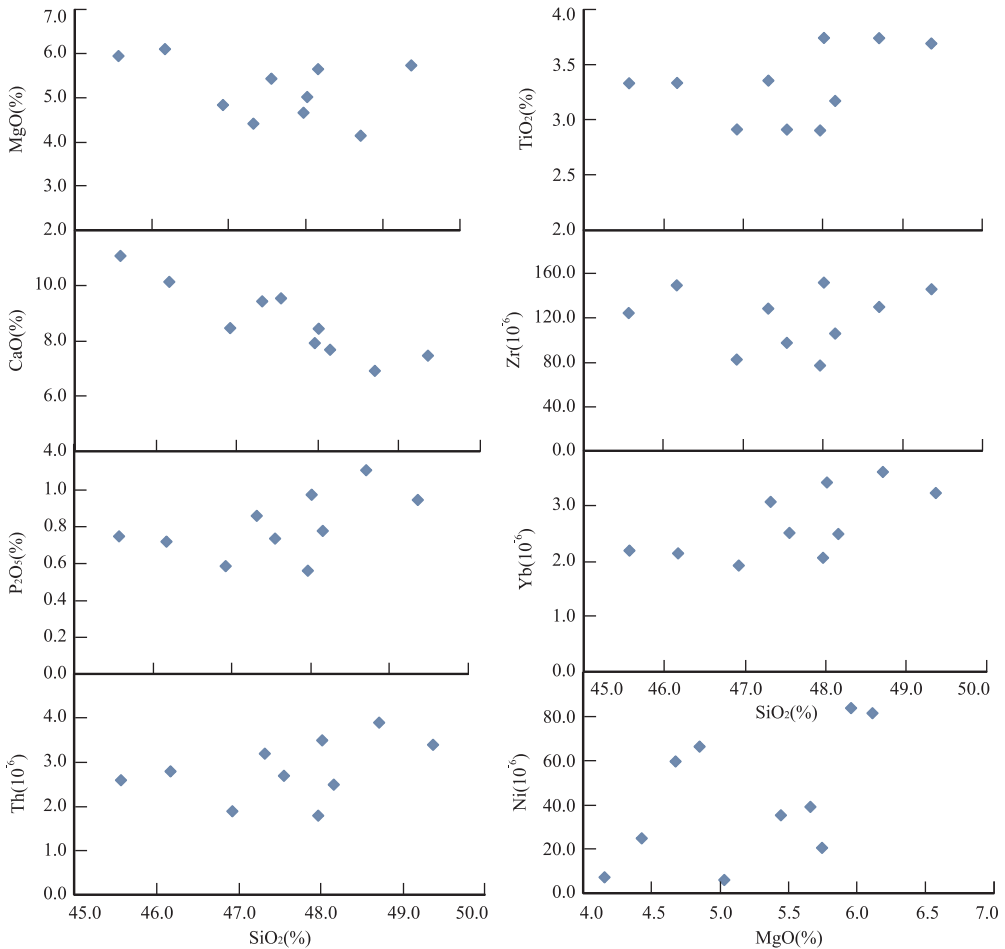


图 5 黔南基性岩墙 Harker 图解

Fig.5 Harker diagrams for the mafic dyke from South Guizhou

高钛玄武岩来自于地幔柱在石榴石稳定域的低度部分熔融(Xu *et al.*, 2001; Song *et al.*, 2001, 2008; Xu *et al.*, 2004; Xiao *et al.*, 2004; Qi *et al.*, 2010); Zhou *et al.*(2006)对云南富宁地区高钛基性岩墙的研究认为其来源于富集的 OIB 型软流圈地

幔低度部分熔融; Xu *et al.*(2007)认为高钛玄武岩来源于岩石圈地幔或者为地幔柱与岩石圈地幔反应形成; Fan *et al.*(2008)通过对广西西部高钛基性岩和玄武岩年代学及地球化学研究,认为其属于峨眉地幔柱的岩浆活动,为含石榴石地幔源区的低度部

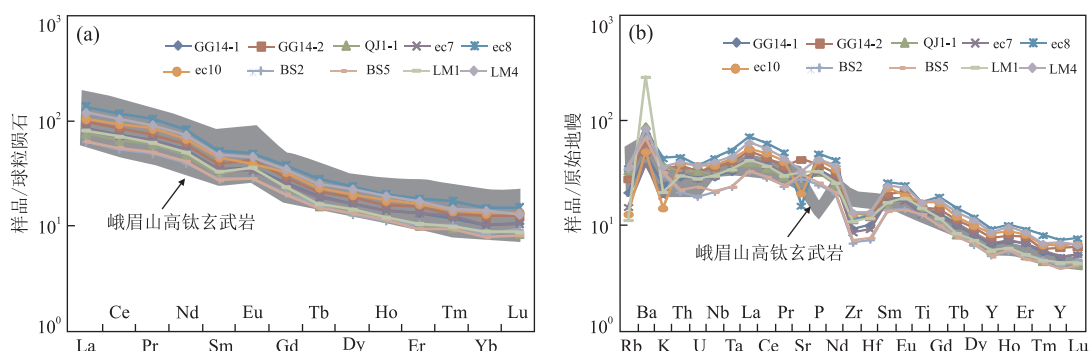


图 6 黔南基性岩墙稀土元素球粒陨石标准化图解(a)和微量元素原始地幔蛛网图(b)

Fig.6 Chondrite-normalized REE patterns (a) and primitive mantle-normalized trace element patterns (b) for the mafic dyke from South Guizhou

图 a 据 Taylor and McLennan(1985);图 b 据 Sun and McDonough(1989).峨眉山高钛玄武岩数据来自 Xu *et al.*(2001); Xiao *et al.*(2003); Zhou *et al.*(2006)

表 2 黔南基性岩墙 Sr-Nd 同位素数据

Table 2 Sr-Nd isotopic data for the mafic dyke from South Guizhou

样品编号	Rb	Sr	$^{87}\text{Rb}/^{86}\text{Sr}$	$^{87}\text{Sr}/^{86}\text{Sr}$	$\pm 2\sigma$	$(^{87}\text{Sr}/^{86}\text{Sr})_i$	Sm	Nd	$^{147}\text{Sm}/^{144}\text{Nd}$	$^{143}\text{Nd}/^{144}\text{Nd}$	$\pm 2\sigma$	$\epsilon_{\text{Nd}}(t)$
GG13	31.7	490	0.187	0.706 582	12	0.706 052	8.21	37.6	0.132 0	0.512 545	10	0.4
GG14-2	18.0	916	0.057	0.706 264	11	0.705 894	8.84	42.8	0.124 9	0.5125 99	6	1.6
GG14-4	16.1	466	0.100	0.706 267	12	0.705 608	8.45	39.5	0.129 3	0.512 587	13	1.3
QJ1-1	21.4	606	0.102	0.705 988	15	0.705 583	7.08	33.6	0.127 4	0.512 509	13	-0.2
QJ1-2	22.1	559	0.114	0.706 008	13	0.705583	6.84	33.2	0.124 6	0.512 491	12	-0.5
QJ1-3	23.0	536	0.124	0.706 045	11	0.705 881	7.00	33.9	0.124 8	0.512 500	10	-0.3
ec11	20.7	561	0.107	0.706 280	13	0.705 278	9.48	42.8	0.133 9	0.512 602	9	1.4
BS5	23.9	663	0.104	0.705 665	13	0.705 405	6.24	28.7	0.131 4	0.512 559	9	0.6
LM4	22.5	708	0.092	0.705 748	15	0.705 888	10.85	51.2	0.128 1	0.512 546	15	0.5
LMZK2	27.5	620	0.128	0.706 365	14	0.706 052	7.47	34.7	0.130 1	0.512 510	11	-0.3

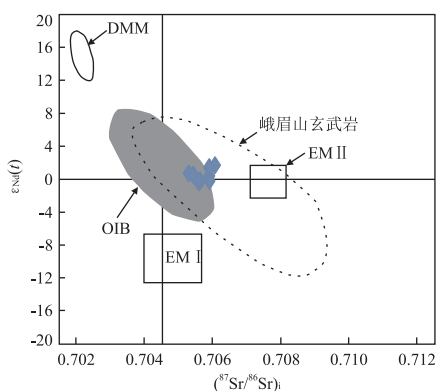


图 7 黔南基性岩墙 Sr-Nd 同位素初始比值

Fig.7 Plot of initial $\epsilon_{\text{Nd}}(t)$ vs. $(^{87}\text{Sr}/^{86}\text{Sr})_i$ for the mafic dyke from South Guizhou

峨眉山玄武岩数据来自 Xu *et al.*(2001); Song *et al.*(2004,2008); Xiao *et al.*(2004); Wang *et al.*(2007); Fan *et al.*(2008); Qi and Zhou(2008); Shellnutt *et al.*(2008).DMM, EMI, EMII 来自 Zindler and Hart(1986); Hart(1988); Weaver(1991)

分熔融,是地幔柱与岩石圈地幔反应成因。

黔南基性岩墙 Harker 图解(图 5)显示 SiO_2 与

MgO 、 CaO 具负相关性, MgO 与 Ni 正相关关系表明基性岩岩浆经历了橄榄石和辉石的分异结晶作用, SiO_2 与中等不相容元素 Zr 、 Th 和 Yb 之间的正相关关系也说明这些元素在分异结晶过程中更易进入熔体中,受橄榄石和辉石的结晶分异影响不大.而 $\text{SiO}_2 (>47\%)$ 与 TiO_2 、 P_2O_5 有正相关关系,在原始地幔标准化蛛网图中(图 6b)基性岩墙 P 为正异常,与峨眉山高钛玄武岩明显的负异常不同,表明岩浆形成演化过程中并没有经历明显的磷灰石和钛铁氧化物的分异结晶.同时, Eu 的正异常暗示了在岩浆演化过程中无长石的分异结晶。

部分微量元素的比值在部分熔融和分异结晶过程中不会发生分异,常用来识别岩浆源区的性质.黔南基性岩墙 Th/Ta (1.80~1.94)、 Nb/U (30.8~39.88)、 Th/La (0.08~0.10)、 Nb/Th (7.89~8.40) 比值与原始地幔 Th/Ta (2.07)、 Nb/U (33.95)、 Th/La (0.12)、 Nb/Th (8.39)相近,表明岩浆形成于与原始地幔相似的地幔橄榄岩部分熔融,其较高 La/Nb 比值(1.25~1.56)显示富集地幔或者地壳物质参与与特

表 3 黔南基性岩墙 SHRIMP 锆石 U-Pb 同位素测定结果

Table 3 SHRIMP U-Pb isotopic compositions of zircons for the mafic dyke from South Guizhou

测点	$^{206}\text{Pb}/^{238}\text{U}$ (%)	含量及比值				同位素比值				同位素年龄(Ma)			不谐和度 (%)		
		U (10^{-6})	Th (10^{-6})	$^{206}\text{Pb}^*$ (10^{-6})	$^{232}\text{Th}/^{238}\text{U}$	$^{207}\text{Pb}^*/^{206}\text{Pb}^*$ 测值 ($\pm\%$)	$^{207}\text{Pb}^*/^{235}\text{U}$ 测值 ($\pm\%$)	$^{206}\text{Pb}^*/^{238}\text{U}$ 测值 ($\pm\%$)	误差 相关系数	$^{206}\text{Pb}/^{238}\text{U}$ 测值 $\pm 1\sigma$	$^{207}\text{Pb}/^{206}\text{Pb}$ 测值 $\pm 1\sigma$				
1.1	0.26	624	587	22.1	0.97	0.050 9	2.0	0.289 0	2.20	0.041 2	1.00	0.451	260.1 \pm 2.6	236 \pm 46	-10
2.1	0.32	148 1	512 2	52.7	3.57	0.050 7	1.8	0.289 2	2.00	0.041 3	0.93	0.455	261.1 \pm 2.4	229 \pm 42	-14
3.1	0.21	203 7	660 2	73.8	3.35	0.051 2	1.3	0.297 3	1.60	0.042 1	0.93	0.579	265.8 \pm 2.4	251 \pm 30	-6
4.1	0.19	619	748	22.2	1.25	0.051 3	1.9	0.295 0	2.10	0.041 7	0.99	0.465	263.4 \pm 2.6	254 \pm 44	-4
5.1	0.14	215 5	360 0	77.4	1.73	0.051 3	1.6	0.295 3	1.80	0.041 7	0.92	0.506	263.5 \pm 2.4	256 \pm 36	-3
6.1	0.08	307 7	328 3	112.0	1.10	0.051 4	0.8	0.299 3	1.20	0.042 2	0.90	0.753	266.7 \pm 2.4	259 \pm 18	-3
7.1	0.20	773	168 5	27.3	2.25	0.051 7	1.7	0.292 4	2.00	0.041 1	0.97	0.494	259.4 \pm 2.5	270 \pm 39	4
8.1	0.14	497	469	17.5	0.98	0.052 4	2.5	0.295 0	2.70	0.040 9	1.00	0.379	258.2 \pm 2.6	301 \pm 57	14
9.1	0.13	118 3	460 3	42.0	4.02	0.051 6	1.4	0.293 5	1.70	0.041 3	0.93	0.553	260.8 \pm 2.4	266 \pm 32	2
10.1	0.94	863	195 1	30.7	2.34	0.050 1	3.4	0.284 0	3.50	0.041 1	0.97	0.275	259.4 \pm 2.5	202 \pm 79	-29

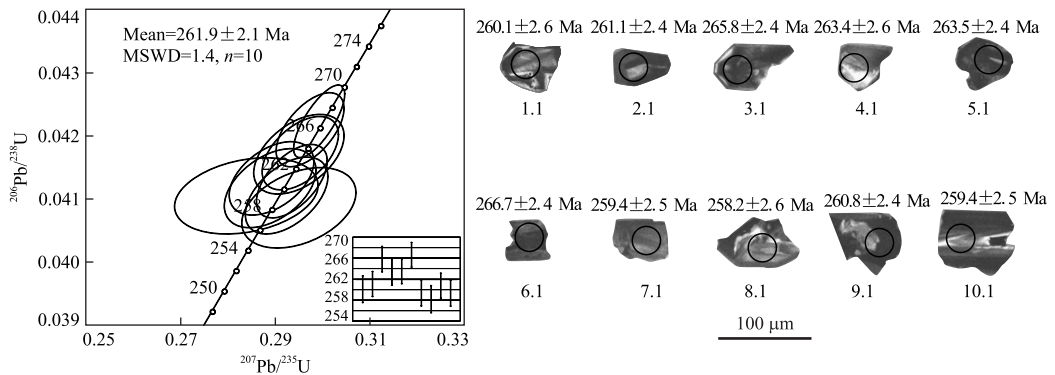


图 8 黔南基性岩墙锆石 U-Pb 年龄谐和图及 CL 图像

Fig.8 Zircon SHRIMP U-Pb concordia diagrams and CL images for the mafic dyke from South Guizhou

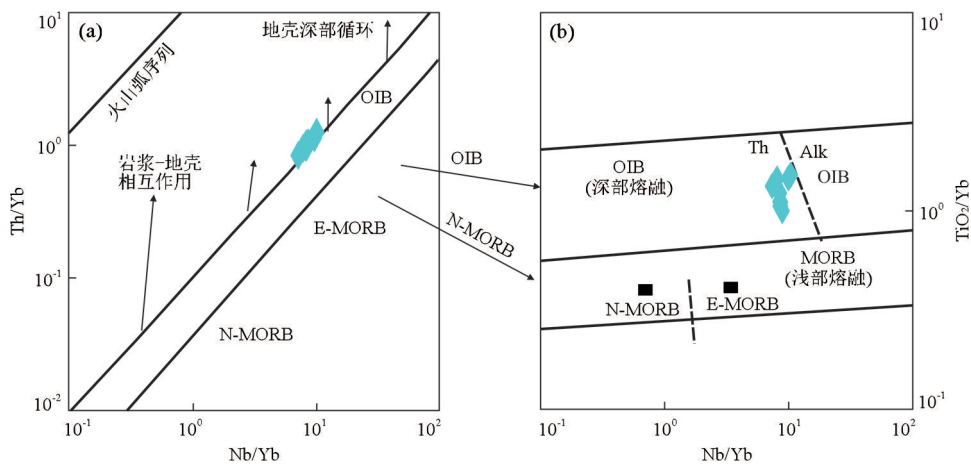


图 9 黔南基性岩墙 Nb/Yb-Th/Yb(a)和 Nb/Yb-TiO₂/Yb(b)图解

Fig.9 Nb/Yb vs. Th/Yb (a) and Nb/Yb vs. TiO₂/Yb (b) diagrams for the mafic dyke from South Guizhou
据 Pearce(2008)

征.在 Th/Yb-Nb/Yb 图解中,所有数据点落入岩浆地幔序列边部,地壳物质混染不明显(图 9a), TiO₂/Yb-Nb/Yb 图解中显示基性岩浆具有 OIB 地

球化学性质(图 9b).基性岩较低的初始(⁸⁷Sr/⁸⁶Sr)_i 比值(0.705 277 5~0.706 052 0),和 ε_{Nd}(t)(-0.5~+1.6),以及较低 Th/Ta 比值(<2.13)显示无明显

表 4 与峨眉山大火成岩省有关的年龄统计

Table 4 Summary of reported age data from the ELIP

年龄(Ma)	测年对象	测年方法	采样地点	文献出处
254±5	辉石岩中的金云母	Ar/Ar	云南大理洱海边	Boven <i>et al.</i> , 2002
251.2~252.8	玄武岩、粗面岩和正长岩	Ar/Ar	云南和四川	Lo <i>et al.</i> , 2002
259±3	辉长岩	SHRIMP	攀西新街侵入岩	Zhou <i>et al.</i> , 2002
253.6±0.4	玄武岩	Ar/Ar	广西百色	Fan <i>et al.</i> , 2004
255.4±0.4	玄武岩	Ar/Ar	广西田阳	Fan <i>et al.</i> , 2004
256.2±0.8	玄武岩	Ar/Ar	广西巴马	Fan <i>et al.</i> , 2004
253.7±6.1	玄武岩	SHRIMP	广西百色	Fan <i>et al.</i> , 2004
262±3	苏长橄榄辉长岩	SHRIMP	四川盐源	Guo <i>et al.</i> , 2004
263±3	淡色辉长岩	SHRIMP	攀枝花侵入岩	Zhou <i>et al.</i> , 2005
260±3	辉绿岩	SHRIMP	云南富宁	Zhou <i>et al.</i> , 2006
258±3	闪长岩	SHRIMP	云南富宁	Zhou <i>et al.</i> , 2006
261.6±4.4	正长岩	SHRIMP	攀西猫猫沟岩体	罗震宇等, 2006
258.9±3.4	玄武岩	Ar/Ar	峨眉山玄武岩省	侯增谦等, 2006
259.3±1.3	矿化辉长岩	TIMS	攀西红格侵入岩	Zhong and Zhu, 2006
260.7±0.8	角闪辉长岩	TIMS	攀西冰谷侵入岩	Zhong and Zhu, 2006
261±4	钠闪石花岗岩	SHRIMP	攀西白马侵入岩附近茨达 A 型花岗岩	Zhong <i>et al.</i> , 2007
251±6	黑云母钾长石花岗岩	SHRIMP	攀西红格侵入岩附近矮郎河 I 型花岗岩	Zhong <i>et al.</i> , 2007
249±32	铜镍硫化物矿石	Re-Os	云南白马寨	Wang <i>et al.</i> , 2007
256.85±2.69	辉长岩中黑云母	Ar/Ar	攀枝花岩体	Wang <i>et al.</i> , 2007
250.2±1.9	苦橄质基性—超基性岩	Ar/Ar	四川丹巴杨柳坪	Wang <i>et al.</i> , 2007
257±4	宣威组底部沉积物	SHRIMP	贵州威宁	He <i>et al.</i> , 2007
260±5	宣威组底部沉积物	SHRIMP	贵州威宁	He <i>et al.</i> , 2007
263±4	玄武岩顶部酸性凝灰岩	SHRIMP	云南洱源	He <i>et al.</i> , 2007
260±4	粘土岩	SHRIMP	四川朝天	He <i>et al.</i> , 2007
263±3	辉长岩	SHRIMP	攀西力马河侵入岩	Zhou <i>et al.</i> , 2008
261±1	闪长岩	SHRIMP	攀西朱布侵入岩	Zhou <i>et al.</i> , 2008
262±2	正长岩	SHRIMP	攀西白马侵入岩	Zhou <i>et al.</i> , 2008
260.6±3.5	蛇纹石化橄榄岩	SHRIMP	云南金宝山岩体	陶琰等, 2008
260.7±5.6	斜长角闪岩	SHRIMP	云南金宝山岩体	陶琰等, 2008
259.6±5.9	斑状玄武岩	SHRIMP	广西巴马	Fan <i>et al.</i> , 2008
259.1±4.0	斑状玄武岩	SHRIMP	广西百色	Fan <i>et al.</i> , 2008
261.6±4.4	霞石正长岩	SHRIMP	攀西猫猫沟侵入岩	Xu <i>et al.</i> , 2008
259.8±3.5	辉石正长岩	SHRIMP	攀西米易	Xu <i>et al.</i> , 2008
260.4±3.6	闪长岩	SHRIMP	攀西米易撒莲镇	Xu <i>et al.</i> , 2008
261.4±2.3	A 型花岗岩	SHRIMP	攀西太和侵入岩	Xu <i>et al.</i> , 2008
266.5±5.1	辉石正长岩	SHRIMP	攀西米易黄草岩体	Xu <i>et al.</i> , 2008
255.2±3.6	过铝质花岗岩	SHRIMP	攀西红格侵入岩附近矮郎河	Xu <i>et al.</i> , 2008
238.4±3.4	流纹凝灰岩	SHRIMP	云南宾川	Xu <i>et al.</i> , 2008
255.0±0.62	辉绿岩	LA-ICP-MS	贵州罗甸	韩伟等, 2009
261±2	辉长岩	SHRIMP	攀西白马侵入岩	Shellnutt <i>et al.</i> , 2009
253.1±1.9	正长岩	SHRIMP	攀枝花侵入岩中正长岩侵入体	Zhong <i>et al.</i> , 2009
259.69±0.61	辉长苏长岩	LA-ICP-MS	攀西大板山	王萌等, 2011
251.0±1.0	凝灰岩	LA-ICP-MS	贵州盘县	朱江等, 2011
260±8	花岗岩	SHRIMP	攀西营盘梁子岩体	Shellnutt <i>et al.</i> , 2011
261±5	镁铁质岩墙	SHRIMP	攀枝花市南部	Shellnutt and Jahn, 2011
259.5±2.7	镁铁质包体	LA-ICP-MS	攀西白马侵入岩	Zhong <i>et al.</i> , 2011
259.0±3.1	镁铁质包体	LA-ICP-MS	攀西白马侵入岩	Zhong <i>et al.</i> , 2011
258.2±2.2	辉长岩	LA-ICP-MS	攀西白马侵入岩	Zhong <i>et al.</i> , 2011
258.5±2.3	正长岩	LA-ICP-MS	攀西白马侵入岩	Zhong <i>et al.</i> , 2011
257.8±2.6	正长岩	LA-ICP-MS	攀西白马侵入岩	Zhong <i>et al.</i> , 2011
256.2±1.5	花岗岩	LA-ICP-MS	攀西白马侵入岩	Zhong <i>et al.</i> , 2011
257.9±2.4	辉长岩	LA-ICP-MS	攀枝花侵入岩	Zhong <i>et al.</i> , 2011
255.4±3.1	辉长岩	LA-ICP-MS	攀枝花侵入岩	Zhong <i>et al.</i> , 2011

续表 4

年龄 (Ma)	测年对象	测年方法	采样地点	文献出处
259.5±1.1	正长闪长岩	LA-ICP-MS	攀枝花侵入岩	Zhong <i>et al.</i> , 2011
259.2±1.3	正长闪长岩	LA-ICP-MS	攀枝花侵入岩	Zhong <i>et al.</i> , 2011
257.8±2.3	正长闪长岩	LA-ICP-MS	攀枝花侵入岩	Zhong <i>et al.</i> , 2011
259.8±1.6	正长闪长岩	LA-ICP-MS	攀枝花侵入岩	Zhong <i>et al.</i> , 2011
255.8±1.8	正长岩	LA-ICP-MS	攀枝花侵入岩	Zhong <i>et al.</i> , 2011
258.7±2.0	辉长岩	LA-ICP-MS	攀西红格侵入岩	Zhong <i>et al.</i> , 2011
258.9±2.1	辉长岩	LA-ICP-MS	攀西红格侵入岩	Zhong <i>et al.</i> , 2011
256.8±2.8	I 型花岗岩	LA-ICP-MS	攀西红格侵入岩	Zhong <i>et al.</i> , 2011
256.2±3.0	I 型花岗岩	LA-ICP-MS	攀西红格侵入岩	Zhong <i>et al.</i> , 2011
258.8±2.3	辉长岩	LA-ICP-MS	攀西太和侵入岩	Zhong <i>et al.</i> , 2011
257.6±0.5	镁铁质侵入岩	CA-TIMS	侵入攀西沃水过铝质正长岩中	Shellnutt <i>et al.</i> , 2012
259.2±0.4	镁铁质岩墙	CA-TIMS	侵入攀西白马侵入岩的过碱性正长岩中	Shellnutt <i>et al.</i> , 2012
259.4±0.8	镁铁质岩墙	CA-TIMS	侵入攀西白马侵入岩的过碱性正长岩中	Shellnutt <i>et al.</i> , 2012
259.6±0.5	准铝质正长岩	CA-TIMS	攀西沃水岩体	Shellnutt <i>et al.</i> , 2012
259.1±0.5	准铝质正长岩	CA-TIMS	攀西大黑山岩体	Shellnutt <i>et al.</i> , 2012
258.9±0.7	准铝质正长岩	CA-TIMS	攀西草黄岩体	Shellnutt <i>et al.</i> , 2012
258.4±0.6	花岗岩	CA-TIMS	攀西白马侵入岩附近茨达	Shellnutt <i>et al.</i> , 2012
257±9	玄武岩	LA-ICP-MS	广西	Lai <i>et al.</i> , 2012
256.7±4.3	基性岩墙	LA-ICP-MS	四川冕宁	Li, 2012
257.6±2	基性岩墙	LA-ICP-MS	云南富民	Li, 2012
255.1±3.6	黑云母二长花岗岩	LA-ICP-MS	侵入攀西红格岩体内部的大老包花岗岩	程黎鹿等, 2013
261.4±4.6	苦橄质岩墙	LA-ICP-MS	攀枝花岩体	Hou <i>et al.</i> , 2013
263±10	辉绿岩	LA-ICP-MS	贵州普安	曾广乾等, 2014
259.1±0.5	长英质熔结凝灰岩	CA-TIMS	云南江尾镇宾川剖面	Zhong <i>et al.</i> , 2014
259.9±1.1	辉长岩	LA-ICP-MS	攀西大板山	Liu <i>et al.</i> , 2015
260.3±1.3	辉长苏长岩	LA-ICP-MS	攀西大板山	Liu <i>et al.</i> , 2015
262~249	花岗岩和流纹岩	LA-ICP-MS	越南北部 Phan Si Pan-Tu Le 地区	Usuki <i>et al.</i> , 2015
264±3	基性岩墙(斜锆石)	SIMS	云南武定	Fan <i>et al.</i> , 2017
256±5	基性岩墙(斜锆石)	SIMS	云南武定	Fan <i>et al.</i> , 2017

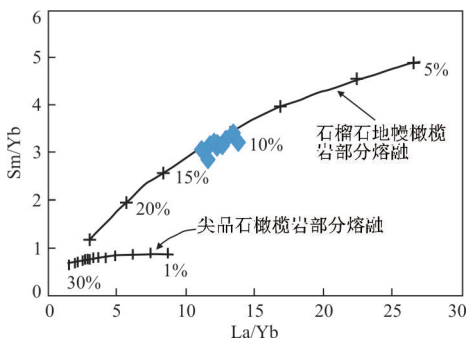


图 10 黔南基性岩 La/Yb-Sm/Yb 图解

Fig.10 La/Yb vs. Sm/Yb diagram for the mafic dyke from South Guizhou

底图引自王妍(2011)

地壳混染。Sr-Nd 同位素位于峨眉山玄武岩分布范围内,具有峨眉山玄武岩亲缘性,明显偏离亏损地幔及地幔序列,位于 OIB 范围及边部,向 EM II 偏移,结合相对亏损的 Nb、Ta、Zr 和 Hf,表明岩浆可能形成于富集地幔源区。Sm/Yb-La/Yb 图解中显示罗甸基性岩可能源于深部石榴石地幔橄榄岩 10%~

12%的部分熔融(图 10)。基性岩 Sr-Nd 同位素特征与峨眉山玄武岩喷发中心区以及东部边缘地区高钛玄武岩和基性岩可对比,地幔柱喷发的边缘地区由于温度较低而岩石圈地幔相对较厚(Xu *et al.*, 2001),地幔柱岩浆在上升过程中可以与周围岩石圈地幔充分反应。因此,黔南基性岩岩浆可能形成于受地幔柱作用的富集石榴石地幔源区 10%~12%部分熔融。

4.2 峨眉山大火成岩省的喷发时限

古地磁证据表明峨眉山玄武岩喷发时限≤1.5 Ma(Huang and Opdyke, 1998; Ali *et al.*, 2002, 2005),Shellnutt *et al.*(2012)采用 CA-TIMS 测年方法对攀西地区与峨眉山玄武岩同期花岗岩以及侵入其中的基性岩墙群精确定年为 257~260 Ma 狭窄范围内,也表明峨眉山大火成岩省活动时间很短,与古地磁证据吻合。朱江等(2011)研究得到贵州盘县峨眉山玄武岩系顶部凝灰岩 LA-ICP-MS 锆石 U-Pb 年龄为 251 Ma,认为其代表了玄武岩的喷发时间,并与 PTB 生物灭绝时间联系起来。不同

测年方法和测年对象得出了不同年龄(表 4),导致研究者对峨眉山玄武岩的喷发时限一直都具有争议。本次测试的基性岩位于峨眉山大火成岩省最东侧,是与玄武岩同源的浅成基性侵入岩,其年龄测试结果与大部分研究者所测的喷发中心的基性侵入岩年龄一致。在大火成岩省分布范围内,基性岩墙或岩床相似的测年结果在云南富宁(Zhou *et al.*, 2006)、四川盐源(Guo *et al.*, 2004)以及攀枝花(Shellnutt and Jahn, 2011)均有报道,但都集中在玄武岩喷发的中心及附近。与罗甸基性岩墙相似的年龄和同位素特征表明,峨眉山大火成岩省外带的岩浆事件可能与主体喷发为同一阶段,并不是喷发的晚期阶段。其年龄代表了大火成岩省的主体喷发年龄,表明峨眉山大火成岩省喷发时间可能在 260 Ma 左右。

自显生宙以来,地球上经历了多次大规模生物灭绝事件,其成因一直是广大学者研究的热点。与火山喷发有关的大火成岩省总是与全球气候变化以及生物灭绝的时间耦合(Stothers, 1993; Wignall, 2001, 2005; Zhou *et al.*, 2002; Schoene *et al.*, 2015),如西伯利亚大火成岩省与二叠纪—三叠纪生物灭绝事件、中大西洋大火成岩省与三叠纪—侏罗纪生物灭绝事件以及印度德干大火成岩省与白垩纪末生物灭绝事件(Bond *et al.*, 2010; Schoene *et al.*, 2015)。由于未能精确限定峨眉山大火成岩省的喷发时间,其与二叠纪的两次生物灭绝事件(瓜德鲁普末期和二叠纪—三叠纪边界)的时间关系一直都存在争议。通过对罗甸基性岩锆石 SHRIMP 精确年龄测试,综合前人对 ELIP 的大量测年结果,认为峨眉山大火成岩省的喷发可能与瓜德鲁普末期生物灭绝有关。

5 结论

(1) 黔南基性岩墙具有与峨眉山高钛玄武岩相似的稀土和微量元素地球化学特征,具有较低的初始($^{87}\text{Sr}/^{86}\text{Sr}$)_i 比值(0.705 278~0.706 052)和 $\epsilon_{\text{Nd}}(t)$ (-0.5~+1.6),岩浆可能形成于受地幔柱作用的富集石榴石地幔源区 10%~12% 的部分熔融,无明显地壳混染。

(2) 黔南基性岩墙 SHRIMP 锆石 U-Pb 年龄为 261.2 ± 2.6 Ma,该岩墙为峨眉山玄武岩的浅成侵入岩,反映了峨眉山大火成岩省的喷发时间可能集中在 260 Ma,综合前人对 ELIP 喷发时限的大量研究结果,认为峨眉山大火成岩省的喷发可能与瓜德鲁

普末期生物灭绝有关。

致谢: 国家科技基础条件平台北京离子探针中心包泽民博士在数据处理方面提供了的大量帮助,审稿专家给出了宝贵的审稿建议,在此一并表示感谢!

References

- Ali, J. R., Lo, C. H., Thompson, G. M., et al., 2004. Emeishan Basalt Ar-Ar Overprint Ages Define Several Tectonic Events That Affected the Western Yangtze Platform in the Mesozoic and Cenozoic. *Journal of Asian Earth Sciences*, 23(2): 163–178. [https://doi.org/10.1016/s1367-9120\(03\)00072-5](https://doi.org/10.1016/s1367-9120(03)00072-5)
- Ali, J. R., Thompson, G. M., Song, X., et al., 2002. Emeishan Basalts (SW China) and the ‘End-Guadalupian’ Crisis: Magnetobiostratigraphic Constraints. *Journal of the Geological Society*, 159(1): 21–29. <https://doi.org/10.1144/0016-764901086>
- Ali, J. R., Thompson, G. M., Zhou, M. F., et al., 2005. Emeishan Large Igneous Province, SW China. *Lithos*, 79(3–4): 475–489. <https://doi.org/10.1016/j.lithos.2004.09.013>
- Bas, M. J. L., Maitre, R. W. L., Streckeisen, A., et al., 1986. A Chemical Classification of Volcanic Rocks Based on the Total Alkali-Silica Diagram. *Journal of Petrology*, 27(3): 745–750. <https://doi.org/10.1093/petrology/27.3.745>
- Belousova, E., Griffin, W., O’Reilly, S. Y., et al., 2002. Igneous Zircon: Trace Element Composition as an Indicator of Source Rock Type. *Contributions to Mineralogy and Petrology*, 143(5): 602–622. <https://doi.org/10.1007/s00410-002-0364-7>
- Bond, D. P. G., Hilton, J., Wignall, P. B., et al., 2010. The Middle Permian (Capitanian) Mass Extinction on Land and in the Oceans. *Earth-Science Reviews*, 102(1): 100–116. <https://doi.org/10.1016/j.earscirev.2010.07.004>
- Boven, A., Pasteels, P., Punzalan, L. E., et al., 2002. $^{40}\text{Ar}/^{39}\text{Ar}$ Geochronological Constraints on the Age and Evolution of the Permo-Triassic Emeishan Volcanic Province, Southwest China. *Journal of Asian Earth Sciences*, 20(2): 157–175. [https://doi.org/10.1016/s1367-9120\(01\)00031-1](https://doi.org/10.1016/s1367-9120(01)00031-1)
- Campbell, I. H., 2007. Testing the Plume Theory. *Chemical Geology*, 241(3–4): 153–176. <https://doi.org/10.1016/j.chemgeo.2007.01.024>
- Chen, F., Hegner, E., Todt, W., 2000. Zircon Ages and Nd Isotopic and Chemical Compositions of Orthogneisses from the Black Forest, Germany: Evidence for a Cambrian Magmatic Arc. *International Journal of Earth Sciences*, 88(4): 791–802. <https://doi.org/10.1007/>

s005310050306

- Chen, F., Siebel, W., Satir, M., et al., 2002. Geochronology of the Karadere Basement (NW Turkey) and Implications for the Geological Evolution of the Istanbul Zone. *International Journal of Earth Sciences*, 91(3): 469–481. <https://doi.org/10.1007/s00531-001-0239-6>
- Chen, W., Wan, Y.S., Li, H.Q., et al., 2011. Isotope Geochronology: Technique and Application. *Acta Geologica Sinica*, 85(11): 1917–1947 (in Chinese with English abstract).
- Cheng, L.L., Zeng, L., Zhang, F., et al., 2013. Mantle-Derived Magmas Underplating and Its Effect on the Crust in the Emeishan Large Igneous Province: Evidence from Geochronological Study and Numerical Simulation of Dalaobao Granites. *Acta Petrologica Sinica*, 29(10): 3533–3539 (in Chinese with English abstract).
- Cheng, Y.Q., 1994. Introduction to Regional Geology of China. Geological Publishing House, Beijing (in Chinese).
- Chung, S.L., Jahn, B.M., 1995. Plume-Lithosphere Interaction in Generation of the Emeishan Flood Basalts at the Permian-Triassic Boundary. *Geology*, 23(10): 889–892. [https://doi.org/10.1130/0091-7613\(1995\)023<0889:pliigo>2.3.co;2](https://doi.org/10.1130/0091-7613(1995)023<0889:pliigo>2.3.co;2)
- Erwin, D. H., 1994. The Permo-Triassic Extinction. *Nature*, 367(6460): 231–236. <https://doi.org/10.1038/367231a0>
- Fan, H.P., Zhu, W.G., Bai, Z.J., et al., 2017. Geochronologic and Geochemical Constraints of the Petrogenesis of Permian Mafic Dykes in the Wuding Area, SW China: Implications for Fe-Ti Enrichment in Mafic Rocks in the ELIP. *Journal of Volcanology and Geothermal Research*, 331: 64–78. <https://doi.org/10.1016/j.jvolgeores.2016.12.005>
- Fan, W.M., Wang, Y.J., Peng, T., et al., 2004. Ar-Ar and U-Pb Geochronology of Late Paleozoic Basalts in Western Guangxi and Its Constraints on the Eruption Age of Emeishan Basalt Magmatism. *Chinese Science Bulletin*, 49(21): 2318–2327. <https://doi.org/10.1360/04wd0201>
- Fan, W.M., Zhang, C.H., Wang, Y.J., et al., 2008. Geochronology and Geochemistry of Permian Basalts in Western Guangxi Province, Southwest China: Evidence for Plume-Lithosphere Interaction. *Lithos*, 102(1/2): 218–236. <https://doi.org/10.1016/j.lithos.2007.09.019>
- Guo, F., Fan, W.M., Wang, Y.J., et al., 2004. When did the Emeishan Mantle Plume Activity Start? Geochronological and Geochemical Evidence from Ultramafic-Mafic Dikes in Southwestern China. *International Geology Review*, 46(3): 226–234. <https://doi.org/10.2747/0020-6814.46.3.226>
- Han, W., Luo, J.H., Fan, J.L., et al., 2009. Late Permian Diabase in Luodian, Southeastern Guizhou, and Its Tectonic Significances. *Geological Review*, 55(6): 795–803 (in Chinese with English abstract).
- Hart, S. R., 1988. Heterogeneous Mantle Domains: Signatures, Genesis and Mixing Chronologies. *Earth and Planetary Science Letters*, 90(3): 273–296. [https://doi.org/10.1016/0012-821x\(88\)90131-8](https://doi.org/10.1016/0012-821x(88)90131-8)
- He, B., Xu, Y.G., Chung, S.L., et al., 2003. Sedimentary Evidence for a Rapid, Kilometer-Scale Crustal Doming Prior to the Eruption of the Emeishan Flood Basalts. *Earth and Planetary Science Letters*, 213(3–4): 391–405. [https://doi.org/10.1016/s0012-821x\(03\)00323-6](https://doi.org/10.1016/s0012-821x(03)00323-6)
- He, B., Xu, Y.G., Huang, X.L., et al., 2007. Age and Duration of the Emeishan Flood Volcanism, SW China: Geochemistry and SHRIMP Zircon U-Pb Dating of Silicic Ignimbrites, Post-Volcanic Xuanwei Formation and Clay Tuff at the Chaotian Section. *Earth and Planetary Science Letters*, 255(3–4): 306–323. <https://doi.org/10.1016/j.epsl.2006.12.021>
- He, H.L., Li, B., Han, L.R., et al., 2002. Evaluation of Determining 47 Elements in Geological Samples by Pressurized Acid Digestion-ICPMS. *Chinese Journal Analysis Laboratory*, 21(5): 8–12 (in Chinese with English abstract).
- Hou, T., Zhang, Z.C., Encarnacion, J., et al., 2013. The Role of Recycled Oceanic Crust in Magmatism and Metallogeny: Os-Sr-Nd Isotopes, U-Pb Geochronology and Geochemistry of Picritic Dykes in the Panzhihua Giant Fe-Ti Oxide Deposit, Central Emeishan Large Igneous Province, SW China. *Contributions to Mineralogy and Petrology*, 165(4): 805–822. <https://doi.org/10.1007/s00410-012-0836-3>
- Hou, Z.Q., Chen, W., Lu, J.R., 2006. The 259Ma Continental Flood Basalt Eruption Event: From the Laser $^{40}\text{Ar}/^{39}\text{Ar}$ Dating Evidence. *Acta Geologica Sinica*, 80(8): 1130 (in Chinese).
- Huang, K.N., Opdyke, N.D., 1998. Magnetostratigraphic Investigations on an Emeishan Basalt Section in Western Guizhou Province, China. *Earth and Planetary Science Letters*, 163(1–4): 1–14. [https://doi.org/10.1016/s0012-821x\(98\)00169-1](https://doi.org/10.1016/s0012-821x(98)00169-1)
- Jin, Y.G., Zhang, J., Shang, Q.H., 1994. Two Phases of the End-Permian Mass Extinction. Pangea: Global Environments and Resources. *Canadian Society of Petroleum Geologists Memoir*, 17: 813–822.
- Lance, P.B., Sandra, L.K., Charlotte, M.A., et al., 2003a. TEMORA 1: A New Zircon Standard for Phanerozoic U-Pb Geochronology. *Chemical Geology*, 200(1–2): 155–170.

- [https://doi.org/10.1016/S0009-2541\(03\)00165-7](https://doi.org/10.1016/S0009-2541(03)00165-7)
- Lance, P. B., Sandra, L. K., Ian, S. W., et al., 2003b. The Application of SHRIMP to Phanerozoic Geochronology; a Critical Appraisal of Four Zircon Standards. *Chemical Geology*, 200 (1 – 2): 171 – 188. [https://doi.org/10.1016/S0009-2541\(03\)00166-9](https://doi.org/10.1016/S0009-2541(03)00166-9)
- Lai, S. C., Qin, J. F., Li, Y. F., et al., 2012. Permian High Ti/Y Basalts from the Eastern Part of the Emeishan Large Igneous Province, Southwestern China: Petrogenesis and Tectonic Implications. *Journal of Asian Earth Sciences*, 47: 216 – 230. <https://doi.org/10.1016/j.jseas.2011.07.010>
- Li, H. B., 2012. Mantle Plume Geodynamic Significances of the Emeishan Large Igneous Province: Evidence from Mafic Dykes, Geochemistry and Stratigraphic Records (Dissertation). China University of Geosciences, Beijing (in Chinese with English abstract).
- Li, H. B., Zhang Z. C., Lü, L. S., 2010. Geometry of the Mafic Dyke Swarms in Emeishan Large Igneous Province: Implications for Mantle Plume. *Acta Petrologica Sinica*, 26 (10): 3143 – 3152 (in Chinese with English abstract).
- Li, H. B., Zhang, Z. C., Richard, E., et al., 2015. Giant Radiating Mafic Dyke Swarm of the Emeishan Large Igneous Province: Identifying the Mantle Plume Centre. *Terra Nova*, 27 (4): 247 – 257. <https://doi.org/10.1111/ter.12154>
- Liu, W. H., Zhang, J., Sun, T., et al., 2015. Low-Ti Iron Oxide Deposits in the Emeishan Large Igneous Province Related to Low-Ti Basalts and Gabbroic Intrusions. *Ore Geology Reviews*, 65: 180 – 197. <https://doi.org/10.1016/j.oregeorev.2014.08.015>
- Lo, C. H., Chung, S. L., Lee, T. Y., et al., 2002. Age of the Emeishan Flood Magmatism and Relations to Permian-Triassic Boundary Events. *Earth and Planetary Science Letters*, 198 (3 – 4): 449 – 458. [https://doi.org/10.1016/S0012-821X\(02\)00535-6](https://doi.org/10.1016/S0012-821X(02)00535-6)
- Ludwig, K. R., 2001. SQUID 1.02. A User's Manual. Berkeley Geochronology Center Special Publication, Berkeley.
- Luo, Z. Y., Xu, Y. G., He, B., et al., 2006. Geochronologic and Petrochemical Evidence for the Genetic Link between the Maomaogou Nepheline Syenites and the Emeishan Large Igneous Province. *Chinese Science Bulletin*, 51 (15): 1802 – 1810 (in Chinese).
- Pearce, J. A., 2008. Geochemical Fingerprinting of Oceanic Basalts with Applications to Ophiolite Classification and the Search for Archean Oceanic Crust. *Lithos*, 100 (1): 14 – 48. <https://doi.org/10.1016/j.lithos.2007.06.016>
- Pearce, J. A., Mei, H. J., 1988. Volcanic Rocks of the 1985 Tibet Geotraverse: Lhasa to Golmud. *Philosophical Transactions of the Royal Society A: Mathematical, Physical and Engineering Sciences*, 327 (1594): 169 – 201. <https://doi.org/10.1098/rsta.1988.0125>
- Qi, H., Xiao, L., Balta, B., et al., 2010. Variety and Complexity of the Late-Permian Emeishan Basalts: Reappraisal of Plume-Lithosphere Interaction Processes. *Lithos*, 119 (1): 91 – 107. <https://doi.org/10.1016/j.lithos.2010.07.020>
- Qi, L., Zhou, M. F., 2008. Platinum-Group Elemental and Sr-Nd-Os Isotopic Geochemistry of Permian Emeishan Flood Basalts in Guizhou Province, SW China. *Chemical Geology*, 248 (1 – 2): 3 – 103. <https://doi.org/10.1016/j.chemgeo.2007.11.004>
- Schoene, B., Samperton, K. M., Eddy, M. P., et al., 2015. U-Pb Geochronology of the Deccan Traps and Relation to the End-Cretaceous Mass Extinction. *Science*, 347 (6218): 182 – 184. <https://doi.org/10.1126/science.aaa0118>
- Shellnutt, J. G., Denyszyn, S. W., Mundil, R., 2012. Precise Age Determination of Mafic and Felsic Intrusive Rocks from the Permian Emeishan Large Igneous Province (SW China). *Gondwana Research*, 22 (1): 118 – 126. <https://doi.org/10.1016/j.gr.2011.10.009>
- Shellnutt, J. G., Jahn, B. M., 2011. Origin of Late Permian Emeishan Basaltic Rocks from the Panxi Region (SW China): Implications for the Ti-Classification and Spatial-Compositional Distribution of the Emeishan Flood Basalts. *Journal of Volcanology and Geothermal Research*, 199 (1): 85 – 95. <https://doi.org/10.1016/j.jvolgeores.2010.10.009>
- Shellnutt, J. G., Jahn, B. M., Zhou, M. F., 2011. Crustally-Derived Granites in the Panzhihua Region, SW China: Implications for Felsic Magmatism in the Emeishan Large Igneous Province. *Lithos*, 123 (1): 145 – 157. <https://doi.org/10.1016/j.lithos.2010.10.016>
- Shellnutt, J. G., Zhou, M. F., Yan, D. P., et al., 2008. Longevity of the Permian Emeishan Mantle Plume (SW China): 1 Ma, 8 Ma or 18 Ma? *Geological Magazine*, 145 (3): 373 – 388. [doi:10.1017/S016756808004524](https://doi.org/10.1017/S016756808004524)
- Shellnutt, J. G., Wang, C. Y., Zhou, M. F., et al., 2009. Zircon Lu-Hf Isotopic Compositions of Metaluminous and Peralkaline A-Type Granitic Plutons of the Emeishan Large Igneous Province (SW China): Constraints on the Mantle Source. *Journal of Asian Earth Sciences*, 35 (1): 45 – 55. <https://doi.org/10.1016/j.jseas.2008.12.003>
- Song, B., Zhang, Y. H., Wan, Y. S., et al., 2002. Mount Making and Procedure of the SHRIMP Dating. *Geological Review*, 48 (Suppl.): 26 – 30 (in Chinese with English abstract).
- Song, X. Y., Qi, H. W., Robinson, P. T., et al., 2008. Melting of the Subcontinental Lithospheric Mantle by the Emeishan Mantle Plume: Evidence from the Basal Alka-

- line Basalts in Dongchuan, Yunnan, Southwestern China. *Lithos*, 100(1): 93—111. <https://doi.org/10.1016/j.lithos.2007.06.023>
- Song, X. Y., Zhou, M. F., Cao, Z. M., et al., 2004. Late Permian Rifting of the South China Craton Caused by the Emeishan Mantle Plume? *Journal of the Geological Society*, 161(5): 773—781. <https://doi.org/10.1144/0016-764903-135>
- Song, X. Y., Zhou, M. F., Hou, Z. Q., et al., 2001. Geochemical Constraints on the Mantle Source of the Upper Permian Emeishan Continental Flood Basalts, Southwestern China. *International Geology Review*, 43(3): 213—225. <https://doi.org/10.1080/00206810109465009>
- Stacey, J. S., Kramers, J. D., 1975. Approximation of Terrestrial Lead Isotope Evolution by a Two-Stage Model. *Earth and Planetary Science Letters*, 26(2): 207—221. [https://doi.org/10.1016/0012-821X\(75\)90088-6](https://doi.org/10.1016/0012-821X(75)90088-6)
- Stothers, R. B., 1993. Flood Basalts and Extinction Events. *Geophysical Research Letters*, 20(13): 1399—1402. <https://doi.org/10.1029/93gl01381>
- Sun, S. S., McDonough, W. F., 1989. Chemical and Isotopic Systematics of Oceanic Basalts; Implications for Mantle Composition and Processes. *Geological Society, London, Special Publications*, 42(1): 313—345. <https://doi.org/10.1144/gsl.sp.1989.042.01.19>
- Tao, Y., Ma, Y. S., Miao, L. C., et al., 2008. SHRIMP U-Pb Zircon Age of the Jinbaoshan Ultramafic Intrusion, Yunnan Province, SW China. *Chinese Science Bulletin*, 53(22): 2828—2832 (in Chinese).
- Taylor, S. R., McLennan, S. M., 1985. The Continental Crust: Its Composition and Evolution. Oxford Press Blackwell, 1—312.
- Usuki, T., Lan, C. Y., Tran, T. H., et al., 2015. Zircon U-Pb Ages and Hf Isotopic Compositions of Alkaline Silicic Magmatic Rocks in the Phan Si Pan-Tu Le Region, Northern Vietnam; Identification of a Displaced Western Extension of the Emeishan Large Igneous Province. *Journal of Asian Earth Sciences*, 97: 102—124. <https://doi.org/10.1016/j.jseaes.2014.10.016>
- Wang, C. Y., Zhou, M. F., Qi, L., 2007. Permian Flood Basalts and Mafic Intrusions in the Jinping (SW China)-Song Da (Northern Vietnam) District; Mantle Sources, Crustal Contamination and Sulfide Segregation. *Chemical Geology*, 243(3—4): 317—343. <https://doi.org/10.1016/j.chemgeo.2007.05.017>
- Wang, D. H., Li, J. K., Liu, F., et al., 2004. Some Problems Related to Mantle Plume and Their Significance in Ore Prospecting. *Acta Geoscientica Sinica*, 25(5): 489—494 (in Chinese with English abstract).
- Wang, M., Zhao, Z. C., Hou, T., et al., 2011. Geochronology and Geochemistry of the Dabanshan Intrusion in Panxi District and Its Constraints on the Metallogenesis of Cu-Ni Sulfide Deposits. *Acta Petrologica Sinica*, 27(9): 2665—2678 (in Chinese with English abstract).
- Wang, S. Y., Zhang, H., Peng, C. L., et al., 2005. Strata of Paleozoic-Mesozoic and Evolution of the Chasmic Furrow in Western Guizhou Province. Geological Publishing House, Beijing, 125—129 (in Chinese).
- Wang, Y., 2011. A Geochemical Study of Cenozoic Continental Basalts from the Subei-Hefei Areas in East-Central China (Dissertation). University of Science and Technology of China, Hefei (in Chinese with English abstract).
- Weaver, B. L., 1991. The Origin of Ocean Island Basalt End-Member Compositions: Trace Element and Isotopic Constraints. *Earth and Planetary Science Letters*, 104(2—4): 381—397. [https://doi.org/10.1016/0012-821X\(91\)90217-6](https://doi.org/10.1016/0012-821X(91)90217-6)
- Wignall, P. B., 2001. Large Igneous Provinces and Mass Extinctions. *Earth-Science Reviews*, 53(1—2): 1—33. [https://doi.org/10.1016/S0012-8252\(00\)00037-4](https://doi.org/10.1016/S0012-8252(00)00037-4)
- Wignall, P. B., 2005. The Link between Large Igneous Province Eruptions and Mass Extinctions. *Elements*, 1(5): 293—297. <https://doi.org/10.2113/gselements.1.5.293>
- Winchester, J. A., Floyd, P. A., 1977. Geochemical Discrimination of Different Magma Series and Their Differentiation Products Using Immobile Elements. *Chemical Geology*, 20: 325—343. [https://doi.org/10.1016/0009-2541\(77\)90057-2](https://doi.org/10.1016/0009-2541(77)90057-2)
- Xiao, L., Xu, Y. G., Chung, S. L., et al., 2003. Chemostratigraphic Correlation of Upper Permian Lavas from Yunnan Province, China; Extent of the Emeishan Large Igneous Province. *International Geology Review*, 45(8): 753—766. <https://doi.org/10.2747/0020-6814.45.8.753>
- Xiao, L., Xu, Y. G., Mei, H. J., et al., 2004. Distinct Mantle Sources of Low-Ti and High-Ti Basalts from the Western Emeishan Large Igneous Province, SW China; Implications for Plume-Lithosphere Interaction. *Earth and Planetary Science Letters*, 228(3—4): 525—546. <https://doi.org/10.1016/j.epsl.2004.10.002>
- Xiao, L., Xu, Y. G., Mei, H. J., et al., 2003. Late Permian Flood Basalts at Jinping Area and Its Relation to Emei Mantle Plume: Geochemical Evidences. *Acta Petrologica Sinica*, 19(1): 38—48 (in Chinese with English abstract).
- Xu, J. F., Suzuki, K., Xu, Y. G., et al., 2007. Os, Pb, and Nd Isotope Geochemistry of the Permian Emeishan Continental Flood Basalts: Insights into the Source of a Large Igneous

- Province. *Geochimica et Cosmochimica Acta*, 71(8): 2104—2119. <https://doi.org/10.1016/j.gca.2007.01.027>
- Xu, Y. G., Chung, S. L., Jahn, B. M., et al., 2001. Petrologic and Geochemical Constraints on the Petrogenesis of Permian-Triassic Emeishan Flood Basalts in Southwestern China. *Lithos*, 58(3): 145—168. [https://doi.org/10.1016/S0024-4937\(01\)00055-X](https://doi.org/10.1016/S0024-4937(01)00055-X)
- Xu, Y. G., He, B., Chung, S. L., et al., 2004. Geologic, Geochemical, and Geophysical Consequences of Plume Involvement in the Emeishan Flood-Basalt Province. *Geology*, 32(10): 917. <https://doi.org/10.1130/G20602.1>
- Xu, Y. G., Luo, Z. Y., Huang, X. L., et al., 2008. Zircon U-Pb and Hf Isotope Constraints on Crustal Melting Associated with the Emeishan Mantle Plume. *Geochimica et Cosmochimica Acta*, 72(13): 3084—3104. <https://doi.org/10.1016/j.gca.2008.04.019>
- Zeng, G. Q., He, L. L., Yang, K. G., 2014. Geochronology, Geochemistry and Geological Significances of Diabase Dykes in Púan, West Guizhou. *Journal of Mineralogy and Petrology*, 34(4): 61—70 (in Chinese with English abstract).
- Zhang, Z., 2006a. Geochemistry of Picritic and Associated Basalt Flows of the Western Emeishan Flood Basalt Province, China. *Journal of Petrology*, 47(10): 1997—2019. <https://doi.org/10.1093/petrology/egl034>
- Zhang, Z., 2006b. Native Gold and Native Copper Grains Enclosed by Olivine Phenocrysts in a Picrite Lava of the Emeishan Large Igneous Province, SW China. *American Mineralogist*, 91(7): 1178—1183. <https://doi.org/10.2138/am.2006.1888>
- Zhang, Z. C., Zhi, X. C., Chen, L., et al., 2008. Re-Os Isotopic Compositions of Picrites from the Emeishan Flood Basalt Province, China. *Earth and Planetary Science Letters*, 276(1—2): 30—39. <https://doi.org/10.1016/j.epsl.2008.09.005>
- Zhong, H., Campbell, I. H., Zhu, W. G., et al., 2011. Timing and Source Constraints on the Relationship between Mafic and Felsic Intrusions in the Emeishan Large Igneous Province. *Geochimica et Cosmochimica Acta*, 75(5): 1374—1395. <https://doi.org/10.1016/j.gca.2010.12.016>
- Zhong, H., Zhu, W. G., 2006. Geochronology of Layered Mafic Intrusions from the Pan-Xi Area in the Emeishan Large Igneous Province, SW China. *Mineralium Deposita*, 41(6): 599—606. <https://doi.org/10.1007/s00126-006-0081-7>
- Zhong, H., Zhu, W. G., Chu, Z. Y., et al., 2007. SHRIMP U-Pb Zircon Geochronology, Geochemistry, and Nd-Sr Isotopic Study of Contrasting Granites in the Emeishan Large Igneous Province, SW China. *Chemical Geology*, 236(1—2): 112—133. <https://doi.org/10.1016/j.chemgeo.2006.09.004>
- Zhong, H., Zhu, W. G., Hu, R. Z., et al., 2009. Zircon U-Pb Age and Sr-Nd-Hf Isotope Geochemistry of the Panzhihua A-Type Syenitic Intrusion in the Emeishan Large Igneous Province, Southwest China and Implications for Growth of Juvenile Crust. *Lithos*, 110(1): 109—128. <https://doi.org/10.1016/j.lithos.2008.12.006>
- Zhong, Y. T., He, B., Mundil, R., et al., 2014. CA-TIMS Zircon U-Pb Dating of Felsic Ignimbrite from the Binchuan Section: Implications for the Termination Age of Emeishan Large Igneous Province. *Lithos*, 204: 14—19. <https://doi.org/10.1016/j.lithos.2014.03.005>
- Zhou, M. F., Arndt, N. T., Malpas, J., et al., 2008. Two Magma Series and Associated Ore Deposit Types in the Permian Emeishan Large Igneous Province, SW China. *Lithos*, 103(3): 352—368. <https://doi.org/10.1016/j.lithos.2007.10.006>
- Zhou, M. F., Malpas, J., Song, X. Y., et al., 2002. A Temporal Link between the Emeishan Large Igneous Province (SW China) and the End-Guadalupian Mass Extinction. *Earth and Planetary Science Letters*, 196(3—4): 113—122. [https://doi.org/10.1016/S0012-821X\(01\)00608-2](https://doi.org/10.1016/S0012-821X(01)00608-2)
- Zhou, M. F., Robinson, P. T., Leshner, C. M., et al., 2005. Geochemistry, Petrogenesis and Metallogenesis of the Panzhihua Gabbroic Layered Intrusion and Associated Fe-Ti-V Oxide Deposits, Sichuan Province, SW China. *Journal of Petrology*, 46(11): 2253—2280. <https://doi.org/10.1093/petrology/egi054>
- Zhou, M. F., Zhao, J. H., Qi, L., et al., 2006. Zircon U-Pb Geochronology and Elemental and Sr-Nd Isotope Geochemistry of Permian Mafic Rocks in the Funing Area, SW China. *Contributions to Mineralogy and Petrology*, 151(1): 1—19. <https://doi.org/10.1007/s00410-005-0030-y>
- Zhu, J., Zhang, Z. C., Hou, T., et al., 2011. LA-ICP-MS Zircon U-Pb Geochronology of the Tuffs on the Uppermost of the Emeishan Basalt Succession in Panxian County, Guizhou Province: Constraints on Genetic Link between Emeishan Large Igneous Province and the Mass Extinction. *Acta Petrologica Sinica*, 27(9): 2743—2751 (in Chinese with English abstract).
- Zindler, A., Hart, S. R., 1986. Chemical Geodynamics. *Annual Review of Earth and Planetary Sciences*, 14: 493—571. <https://doi.org/10.1146/annurev.earth.14.050186.002425>

附中文参考文献

- 陈文, 万渝生, 李华芹, 等, 2011. 同位素地质年龄测定技术及应用. *地质学报*, 85(11): 1917—1947.

- 程黎鹿,曾铃,张帆,等,2013.峨眉山大火成岩省幔源岩浆底侵作用的地壳响应:来自大老包花岗岩的年代学和热模拟证据.岩石学报,29(10): 3533-3539.
- 程裕淇,1994.中国区域地质概论.北京:地质出版社.
- 韩伟,罗金海,樊俊雷,等,2009.贵州罗甸晚二叠世辉绿岩及其区域构造意义.地质论评,55(6): 795-803.
- 何红蓼,李冰,韩丽荣,等,2002.封闭压力酸溶-ICP-MS 法分析地质样品中 47 个元素的评价.分析试验室,21(5): 8-12.
- 侯增谦,陈文,卢记仁,2006.四川峨眉山大火成岩省 259 Ma 大陆溢流玄武岩喷发事件:来自激光 $^{40}\text{Ar}/^{39}\text{Ar}$ 测年证据.地质学报,80(8): 1130.
- 李宏博,2012.峨眉山大火成岩省地幔柱动力学:基性岩强墙群、地球化学及沉积地层学证据(博士学位论文).北京:中国地质大学.
- 李宏博,张招崇,吕林素,2010.峨眉山大火成岩省基性墙群几何学研究及对地幔柱中心的指示意义.岩石学报,26(10): 3143-3152.
- 罗震宇,徐义刚,何斌,等,2006.论攀西猫猫沟霞石正长岩与峨眉山大火成岩省的成因联系:年代学和岩石地球化学证据.科学通报,51(15): 1802-1810.
- 宋彪,张玉海,万渝生,等,2002.锆石 SHRIMP 样品靶制作,年龄测定及有关地质现象讨论.地质论评,48(增刊): 26-30.
- 陶琰,马言胜,苗来成,等,2008.云南金宝山超镁铁岩体锆石 SHRIMP 年龄.科学通报,53(22): 2828-2832.
- 王登红,李建康,刘峰,等,2004.地幔柱研究中几个问题的探索及其找矿意义.地球学报,25(5): 489-494.
- 王萌,张招崇,侯通,等,2011.攀西地区大板山岩体的年代学、元素地球化学及其对铜镍硫化物矿床成因的约束.岩石学报,27(9): 2665-2678.
- 王尚彦,张慧,彭成龙,等,2005.贵州西部古一中生代地层及裂隙槽盆的演化.北京:地质出版社.
- 王妍,2011.中国东部苏北-合肥新生代大陆玄武岩地球化学研究(博士学位论文).合肥:中国科学技术大学.
- 肖龙,徐义刚,梅厚钧,等,2003.云南金平晚二叠纪玄武岩特征及其与峨眉山地幔柱关系——地球化学证据.岩石学报,19(1): 38-48.
- 曾广乾,何良伦,杨坤光,2014.黔西普安辉绿岩的年代学、地球化学特征及其地质意义.矿物岩石,34(4): 61-70.
- 朱江,张招崇,侯通,等,2011.贵州盘县峨眉山玄武岩系顶部凝灰岩 LA-ICP-MS 锆石 U-Pb 年龄:对峨眉山大火成岩省与生物大规模灭绝关系的约束.岩石学报,27(9): 2743-2751.